

## WTS-2 b: Too close for comfort?

J.L. Birkby<sup>1,a</sup>, M. Cappetta<sup>2</sup>, P. Cruz<sup>3</sup>, J. Koppenhoefer<sup>4</sup>, O. Ivanyuk<sup>5</sup>,  
A. Mustill<sup>6</sup>, S.T. Hodgkin<sup>7</sup>, D.J. Pinfield<sup>8</sup>, B. Sipócz<sup>8</sup>, G. Kovács<sup>7</sup>, R. Saglia<sup>2</sup>,  
Y. Pavlenko<sup>5</sup> and the RoPACS collaboration

<sup>1</sup>Leiden Observatory, Leiden University, Niels Bohrweg 2, 2333 CA Leiden, The Netherlands

<sup>2</sup>Max-Planck-Institut für extraterrestrische Physik, Giessenbachstrasse, 85741 Garching, Germany

<sup>3</sup>Departamento de Astrofísica, Centro de Astrobiología (CSIC/INTA), PO Box 78, 28691 Villanueva de la Cañada, Spain

<sup>4</sup>Universitätssternwarte Scheinerstrasse 1, 81679 München, Germany

<sup>5</sup>Main Astronomical Observatory of Ukrainian Academy of Sciences, Golosiiv Woods, Kyiv-127, 03680, Ukraine

<sup>6</sup>Departamento de Física Teórica, Facultad de Ciencias, Universidad Autónoma de Madrid, Cantoblanco, 28049 Madrid, España

<sup>7</sup>Institute of Astronomy, University of Cambridge, Madingley Road, Cambridge CB3 0HA, UK

<sup>8</sup>Centre for Astrophysics Research, University of Hertfordshire, College Lane, Hatfield, Hertfordshire AL10 9AB, UK

**Abstract.** We report the discovery of WTS-2 b, a typical hot Jupiter in an unusually close 1.02-day orbit to a K-dwarf star. This is the second planet to be discovered in the infrared light curves of the WFCAM Transit Survey (WTS) and is only one-and-a-half times the separation from its host star at which it would be destroyed by Roche lobe overflow. The predicted remaining lifetime of the planet is just 38 Myrs, assuming a tidal dissipation quality factor of  $Q'_* = 10^6$ . The magnitude of  $Q'_*$  is largely unconstrained by observations, thus WTS-2 b provides a useful calibration point for theories describing how frictional processes within a host star affect the tidal orbital evolution of its companion giant planets. It is expected that stars with large convective envelopes are more efficient at dissipating the orbital energy of the planet, and WTS-2 b provides an observational constraint in the sparsely populated K-dwarf regime. In addition, despite its relatively faint magnitude, the favourable size ratio of the WTS-2 star-planet system and the predicted hot equilibrium temperature of the planet will make it possible to characterise the planet's atmosphere via secondary eclipse measurements using existing ground-based instrumentation.

### 1. INTRODUCTION

The orbital period distribution of hot Jupiters ( $a < 0.1$  AU) is not smooth. There is a “pile-up” of planets between  $\sim$ 3–4 days, with a sharp drop-off at longer and shorter periods. The former can be partly attributed to a lack of sensitivity in transit surveys, but the short period drop-off is a genuine feature of the distribution [1, 2]. Only a handful of hot Jupiters have sub-0.02 AU orbits ( $\lesssim$  1-day), which has lead to the conclusion that these rare planets are either difficult to get into such short orbits, or that once they arrive they are quickly destroyed by strong tidal forces [3]. In the latter case, the planets are predicted to have short remaining lifetimes as they will quickly reach their Roche lobe overflow separation, so

---

<sup>a</sup>e-mail: [birkby@strw.leidenuniv.nl](mailto:birkby@strw.leidenuniv.nl)

This is an Open Access article distributed under the terms of the Creative Commons Attribution License 2.0, which permits unrestricted use, distribution, and reproduction in any medium, provided the original work is properly cited.

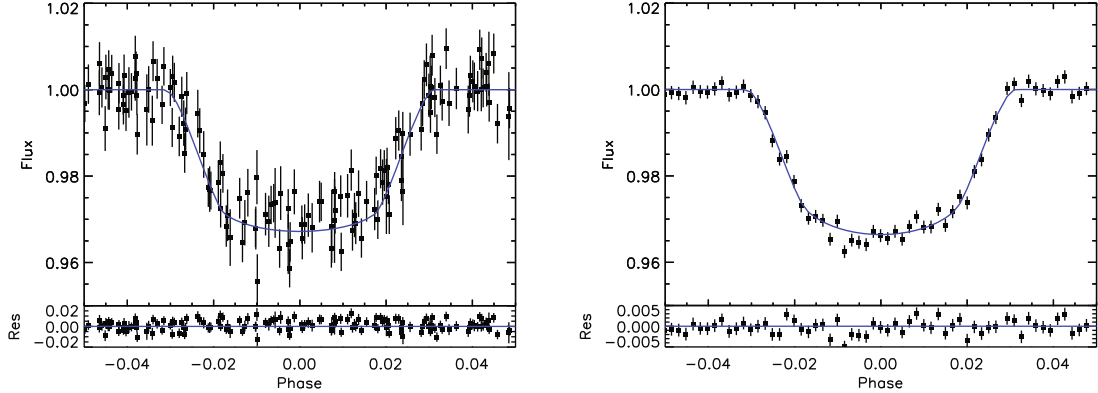


**Figure 1.** Transit light curves of WTS-2 b from the WTS *J*-band (left) and the INT *i*-band (right). The blue solid line shows the best model fit to the data from a simultaneous fitting of the two light curves. The lower panels show the residuals to the model.

those with old host stars are thus seen in the last and transient stage of their orbital evolution. This is under the assumption that the efficiency with which the energy of the orbit is dissipated by frictional processes within the star is of order  $Q'_* = 10^6$  [4, 5]. The magnitude of  $Q'_*$  is the subject of much debate and is largely unconstrained by observations. Theories have been developed to reduce the efficiency of the stellar tidal dissipation in order to extend the remaining lifetimes of the closest hot Jupiters (e.g. [6, 7]), such that their detection is more likely i.e. not in a transient phase. Of the shortest remaining lifetime systems, a number orbit hot stars ( $M_* > 1M_\odot$ ), whose convective envelopes are relatively small compared to the cooler K- and M-dwarfs. It has been suggested that the mass of the convective envelope plays an important role in the efficiency of tidal dissipation, with cooler, more convective stars being the more efficient [8–11]. This calls for a direct observational constraint on  $Q'_*$  as a function of stellar type, which can be achieved on reasonable timescales by measuring the rate of orbital decay in very close orbit hot Jupiters. We present here WTS-2 b, the second planet from the WFCAM Transit Survey (WTS), and one that could provide such a constraint in the K-dwarf regime.

## 2. OBSERVATIONS AND CHARACTERISATION OF THE WTS-2 B SYSTEM

The WTS is an ongoing photometric monitoring campaign that operates as a poor weather program on the 3.8 m United Kingdom Infrared Telescope (UKIRT) on Mauna Kea, Hawaii. The survey uses the Wide-Field Camera (WFCAM) to observe at infrared wavelengths (*J*-band,  $1.25\ \mu\text{m}$ ) and covers  $\sim 6$  square degrees of the sky spread across four fields, where at least one field is visible at any time. For more details on the survey, the reduction of the *J*-band light curves, and the method for identifying transiting planet candidates, see these proceedings, or [12, 13], and [14]. The transit of WTS-2 b as seen in the *J*-band WTS light curve, phase folded on the detected 1.02-day period, is shown in Figure 1 along with a follow-up *i*-band transit from the Isaac Newton Telescope (INT). The light curves are used to simultaneously constrain the best-fitting analytic transit model [15], which is shown by the solid lines.

Follow-up intermediate- and high-resolution spectra were obtained with TWIN at the Calar Alto Observatory (CAHA) and HRS at the Hobby Eberly Telescope (HET), respectively, in order to characterise the host star and to measure its radial velocity curve. The TWIN spectra ( $\sim 6200 - 6950\ \text{\AA}$ ) were extracted using standard IRAF procedures, and the echelle spectra ( $\sim 4400 - 6280\ \text{\AA}$ ) from HRS were extracted following [16] and [14]. The host star is relatively faint ( $V = 15.9$  mag,  $i_{\text{SDSS}} = 15.2$  mag, and  $J_{\text{2MASS}} = 13.9$  mag) such that the high resolution spectra do not have sufficient

## Hot Planets and Cool Stars

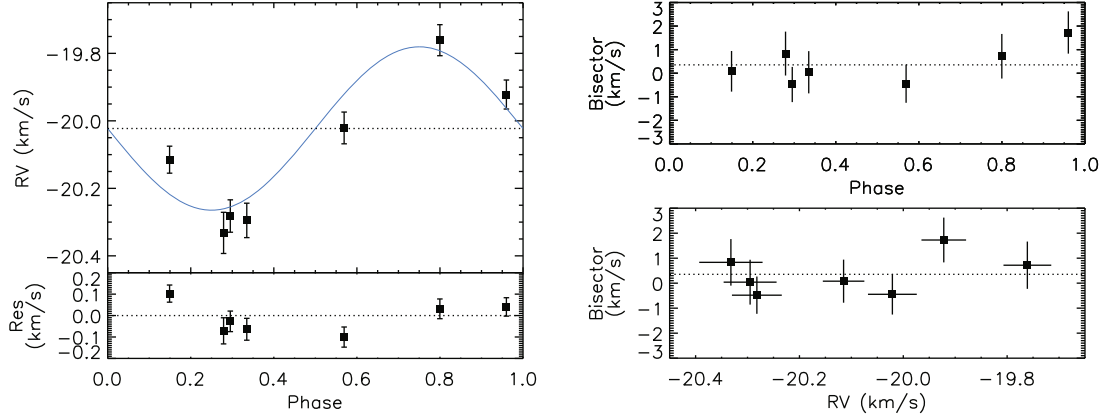


**Figure 2.** *Left:* the radial velocity curve of WTS-2 based on the analysis of high-resolution HRS/HET spectra. The solid blue line is the best-fitting model and the dotted horizontal line marks the systemic velocity of the system. The lower panel gives the residuals to the model. *Right:* line bisectors as a function of phase (upper panel) and radial velocity (lower panel). The lack of correlation and the scatter around zero is evidence against a blend scenario.

signal-to-noise to characterise the star using the standard methods [17]. Instead, we combine results from i) a fit to the spectral energy distribution of the star using all the available broadband photometry in the VOSA data base [18], ii) fitting synthetic spectra to the TWIN spectra, and iii) a spectroscopic abundance analysis of the Fe I and Fe II lines in the HRS spectra. We find a star consistent with  $T_{\text{eff}} = 5000 \pm 250$  K, a slight super-solar metallicity ( $[\text{Fe}/\text{H}] \sim 0.2$ ), slow rotation ( $v \sin(i) = 2.2 \pm 1.0$  km/s), and a lithium abundance  $\log N(\text{Li}) < 1.8$  dex. The lithium constraint, combined with the model isochrones from the PARSEC stellar evolution code [19], give a lower age limit of  $> 600$  Myrs,  $M_{\star} = 0.82 M_{\odot}$ , and  $R_{\star} = 0.761 R_{\odot}$ , consistent with a K2V star. Combined with the radius ratio from the best-fitting light curve model, the planet radius is  $R_P = 1.300 \pm 0.058 R_J$ , i.e. slightly inflated, but very typical for the hot Jupiter population. The radial velocities (RVs) measured from the HRS spectra are shown in Figure 2, along with the line bisectors. A  $\chi^2$  fit of a simple sinusoid (i.e. circular orbit) to the RVs results in a semi-amplitude of  $K = 256 \pm 24$  m/s, resulting in a planet mass of  $M_P = 1.12 \pm 0.13 M_J$ .

The lack of correlation between the line bisectors and phase or RV is evidence against a blend scenario, although the scatter is too large to draw a firm conclusion. Although WFCAM has a small pixel scale (0.4"/pix), the WTS still suffers from blending, so we performed further tests to rule out a false positive. Firstly, the measured transit depths in the *J*- and *i*-band only vary by  $\sim 0.1\%$ , hence any blending background eclipsing binary would need to have the same spectral type as the foreground K-dwarf, and a similar systemic velocity to avoid detection in the HRS spectra. Secondly, to assess the amount of third light from a single background star that could dilute the depth of the transit of the foreground K-dwarf, we re-ran our simultaneous *J*- and *i*-band light curve modelling MCMC simulations allowing for a wide range of possible background blending spectral types, while fixing the foreground star to 5000 K and  $R_{\star} = 0.761 R_{\odot}$ . We find that significant third light is only possible for blending sources with spectral types similar to the foreground star or redder. The  $1\sigma$  upper limit on the third light is 42%, leading to an enlarged planet radius of  $1.72 R_J$ . This is still within the range of radii for the most inflated hot Jupiters, and we note that it is difficult to rule out this type of blending scenario for many of the published exoplanets. The full parameters of the star-planet system are given in Table 1.

### 3. TIDAL DISSIPATION

The most notable property of this otherwise typical hot Jupiter is its orbital separation of just  $a = 0.01855$  AU. Its close proximity to its host star suggests that its orbital evolution is dominated by

**Table 1.** Parameters for the WTS-2 b system. <sup>a</sup>From spectroscopic analysis. <sup>b</sup>From light curve mean stellar density and stellar evolution isochrones. <sup>c</sup>From light curve analysis.  $\xi$  is the stellar microturbulence. The proper motions  $\mu_x \cos \delta$  and  $\mu_{\text{delta}}$  are from the SDSS DR9 database. The space velocities  $U, V, W$  are with respect to the Sun (heliocentric) but for a left-handed coordinate system, i.e. U is positive away from the Galactic centre. <sup>d</sup>Equilibrium temperature assuming  $A_B = 0$  and  $f = 2/3$ .  $a_{\text{Roche}}$  is the Roche limit i.e. the critical distance inside which the planet would begin to lose mass.  $g_b$  is the planet surface gravity according to equation 7 of [20].  $\Theta$  is the Safronov number [21]. The errors on the light curve parameters are the 68.3% confidence interval while the parameter value is the mean of the 68.3% confidence level boundaries, such that the errors are symmetric.

Stellar properties:	System properties:
Name WTS-2	$P$ $1.0187071 \pm 7.1 \times 10^{-7}$ days
$T_{\text{eff}}$ $5000 \pm 250$ K	$T_0$ $2454317.81303 \pm 7.1 \times 10^{-4}$ HJD
Spectral Type K2( $\pm 2$ )V	$R_p/R_{\star}$ $0.1755 \pm 0.0018$
$\log(g)^a$ $4.5 \pm 0.5$	$b$ $0.598 \pm 0.032$
$\log(g)^b$ $4.589 \pm 0.23$	$i$ $83.43 \pm 0.53$ °
[Fe/H] $0.2^{+0.3}_{-0.2}$	$a$ $0.01855 \pm 0.00062$ AU ( $1.51 \pm 0.11 a_{\text{Roche}}$ )
$v \sin(i)$ $2.2 \pm 1.0$ km/s	$K$ $256 \pm 24$ m/s
$\xi$ $0.75 \pm 0.5$ km/s	$V_{\text{sys}}$ (km/s) $-20.026 \pm 0.019$ km/s
$\log N(Li)$ $< 1.8$ dex	$e$ 0 (fixed)
$M^b$ $0.820 \pm 0.082 M_{\odot}$	Planet properties:
$R_{\star}^b$ $0.761 \pm 0.033 R_{\odot}$	$M_p$ $1.12 \pm 0.13 M_J$
$\rho_{\star}^c$ $1.86 \pm 0.15 \rho_{\odot}$	$R_p$ $1.300 \pm 0.058 R_J$
$R_{cz}$ $0.54 \pm 0.04 R_{\odot}$	$\rho_p$ $0.63 \pm 0.11 \text{ g cm}^{-3}$ ( $0.477 \pm 0.084 \rho_J$ )
$M_{cz}$ $\sim 0.05 M_{\odot}$	$g_b$ $16.4 \pm 2.4 \text{ ms}^{-2}$
Age $> 600$ Myr	$F_{\text{inc}}$ $1.29 \times 10^9 \pm 0.29 \times 10^{-9}$ erg/s/cm <sup>2</sup>
$A_V$ $0.27 \pm 0.07$ mag	$T_{\text{eq}}^d$ $2000 \pm 100$ K
Distance $\sim 1$ kpc	$\Theta$ $0.0390 \pm 0.0063$
$\mu_x \cos \delta$ $2.3 \pm 2.3$ mas/yr	
$\mu_{\text{delta}}$ $-1.9 \pm 2.3$ mas/yr	
$U$ $-13.3 \pm 5.6$ km/s	
$V$ $-0.3 \pm 7.7$ km/s	
$W$ $-15.1 \pm 5.3$ km/s	

tidal forces. The tide raised on the star by the planet exerts a strong torque that transfers the angular momentum of the planetary orbit to the stellar spin. For WTS-2 b, the total angular momentum in the system is not sufficient to reach equilibrium [22] and the planet will continue to spiral in until it is presumably destroyed by Roche lobe overflow [23]. We have estimated a timescale for the planet's demise by adopting a simple model of tidal interactions, namely the damping of the equilibrium tide by viscous forces inside the star, with the tidal bulge lagging the planet by a constant time [22, 24, 25]. The model is dependent only on the planetary mean motion and stellar spin, and we have assumed that the efficiency of the tidal dissipation within the host star, as described by the quality factor  $Q'_*$ , is of order  $10^6$ , similar to that found for stellar binaries [4]. Following the prescription of [22], while assuming a non-rotating host star and a circular orbit, we find that integrating their equation 7 gives a remaining lifetime for WTS-2 b of just  $\sim 38$  Myrs. The orbital evolution can be translated into an expected shift in the transit arrival time of the planet due to its decaying orbit (see [14] for equations). We find that under our adopted model, with  $Q'_* = 10^6$ , we expect to see the transit of WTS-2 b arrive  $\sim 18$  seconds earlier after 15 years since its discovery compared to that predicted for a stable orbit. This is observationally feasible to detect if we assume a nominal timing accuracy of  $\sim 5$  seconds [26]. Figure 3 shows the expected shift in the transit arrival time for some of the closest known hot Jupiters after 10 years, again assuming  $Q'_* = 10^6$ . If  $Q'_*$  is dependent on the internal structure of the host star, then after 10 years if

## Hot Planets and Cool Stars

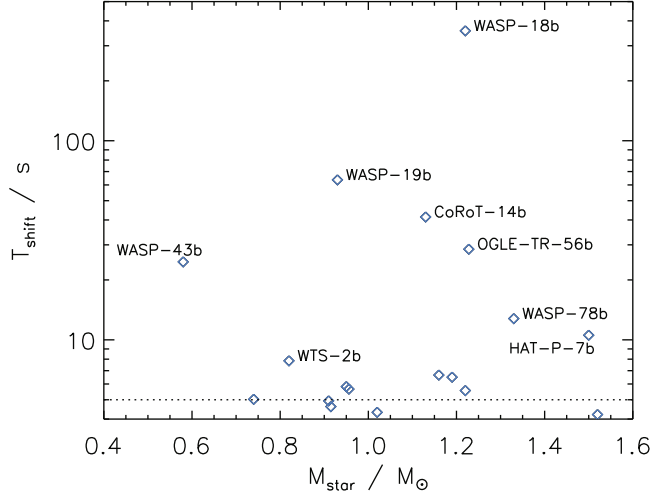


**Figure 3.** Expected change in transit arrival time ( $T_{\text{shift}}$ ) for known transiting hot Jupiters after 10 years assuming  $Q'_* = 10^6$  in our adopted model. The planets shown have near circular orbits ( $e < 0.0093$ ), masses  $M_P > 0.3M_J$ , and host stars that rotate slower than the planetary orbital period to ensure inspiral (data from exoplanets.org). The horizontal dotted line marks a nominal 5 second timing accuracy. After 10 years, strong observational constraints on the lower limit of  $Q'_*$  would be available across a wide range of stellar internal structure.

no change is seen in the transit arrival times of these planets, strong observational constraints can be placed on the lower limit of  $Q'_*$  as a function of stellar mass.

## 4. FOLLOW-UP POTENTIAL

Despite the relative faintness of the host star, the fact that WTS-2 b is very hot and orbits a relatively small star, means that its secondary eclipse depths will be deeper compared to other Jupiters of similar  $T_{\text{eq}}$  that orbit more luminous stars. This makes the planet favourable for follow-up characterisation of its atmosphere, and would provide an insight into the influence of the host star spectrum on the composition and structure of highly irradiated hot Jupiter atmospheres. To assess the potential of ground-based follow-up studies of WTS-2 b's atmosphere, we first calculate the expected equilibrium temperature of the planet [27], assuming a zero-albedo ( $A_B = 0$ , no reflection), no advection of energy from the day-side to the night-side ( $f = 2/3$ ), and that the star and planetary spectra can be approximated as black-bodies. We find an expected equilibrium temperature of  $T_{\text{eq}} = 2000 \pm 100$  K. Adopting this value as the maximum day-side temperature of the planet, we predict the following secondary eclipse depths in the IZJHKs-bands:  $(F_P/F_{\star})_I \sim 0.14 \times 10^{-3}$ ,  $(F_P/F_{\star})_Z \sim 0.19 \times 10^{-3}$ ,  $(F_P/F_{\star})_J \sim 0.82 \times 10^{-3}$ ,  $(F_P/F_{\star})_H \sim 1.7 \times 10^{-3}$ , and  $(F_P/F_{\star})_{K_s} \sim 3.0 \times 10^{-3}$ , respectively. Under our assumptions, the  $K_s$ -band predicted secondary eclipse is one of the deepest expected secondary eclipses amongst the population of known hot Jupiters, and ground-based studies have shown that it is possible to detect these events at similar host star magnitudes [28–30].

All authors of this paper have received support from the RoPACS network during this research, a Marie Curie Initial Training Network funded by the European Commission's Seventh Framework Programme.

## References

- [1] A.W. Howard, G.W. Marcy, S.T. Bryson, J.M. Jenkins, J.F. Rowe, N.M. Batalha, W.J. Borucki, D.G. Koch, E.W. Dunham, T.N. Gautier, III et al., ApJSupp, **201**, 15 (2012), 1103.2541
- [2] C. Hellier, D.R. Anderson A. Collier Cameron, A.P. Doyle, A. Fumel, M. Gillon, E. Jehin, M. Lendl, P.F.L. Maxted, F. Pepe et al., MNRAS, **426**, 739 (2012), 1204.5095
- [3] C. Hellier, D.R. Anderson, A. Collier-Cameron, G.R.M. Miller, D. Queloz, B. Smalley, J. Southworth, A.H.M.J. Triaud, ApJ, **730**, L31 (2011), 1101.3293
- [4] S. Meibom, R.D. Mathieu, ApJ, **620**, 970 (2005), arXiv:astro-ph/0412147
- [5] B. Jackson, R. Greenberg, R. Barnes, ApJ, **678**, 1396 (2008), 0802.1543
- [6] G.I. Ogilvie, D.N.C. Lin, ApJ, **661**, 1180 (2007), arXiv:astro-ph/0702492
- [7] S.L. Li, N. Miller, D.N.C. Lin, J.J. Fortney, Nature, **463**, 1054 (2010), 1002.4608
- [8] A.J. Barker, G.I. Ogilvie, MNRAS, **395**, 2268 (2009), 0902.4563
- [9] A.J. Barker, G.I. Ogilvie, MNRAS, **404**, 1849 (2010), 1001.4009
- [10] J.N. Winn, D. Fabrycky, S. Albrecht, J.A. Johnson, ApJ, **718**, L145 (2010), 1006.4161
- [11] K. Penev, D. Sasselov, ApJ, **731**, 67 (2011), 1102.3187
- [12] G. Kovacs, S. Hodgkin, B. Sipocz, D. Pinfield, D. Barrado, J. Birkby, M. Cappetta, P. Cruz, J. Koppenhoefer, E. Martin et al., MNRAS, (*submitted* 2012)
- [13] J. Birkby, B. Nefs, S. Hodgkin, G. Kovács, B. Sipőcz, D. Pinfield, I. Snellen, D. Mislis, F. Murgas, N. Lodieu et al., MNRAS, **426**, 1507 (2012), 1206.2773
- [14] J.L. Birkby, et al., submitted to MNRAS (2013)
- [15] K. Mandel, E. Agol, ApJ, **580**, L171 (2002), arXiv:astro-ph/0210099
- [16] M. Cappetta, R.P. Saglia, J.L. Birkby, J. Koppenhoefer, D.J. Pinfield, S.T. Hodgkin, P. Cruz, G. Kovács, B. Sipőcz, D. Barrado et al., MNRAS, **427**, 1877 (2012), 1210.1217
- [17] G. Torres, D.A. Fischer, A. Sozzetti, L.A. Buchhave, J.N. Winn, M.J. Holman, J.A. Carter, ApJ, **757**, 161 (2012), 1208.1268
- [18] A. Bayo, C. Rodrigo, D. Barrado Y Navascués, E. Solano, R. Gutiérrez, M. Morales-Calderón, F. Allard, A&A, **492**, 277 (2008), 0808.0270
- [19] A. Bressan, P. Marigo, L. Girardi, B. Salasnich, C. Dal Cero, S. Rubele, A. Nanni, MNRAS, **427**, 127 (2012), 1208.4498
- [20] J. Southworth, MNRAS, **386**, 1644 (2008), 0802.3764
- [21] B.M.S. Hansen, T. Barman, ApJ, **671**, 861 (2007), 0706.3052
- [22] S. Matsumura, S.J. Peale, F.A. Rasio, ApJ, **725**, 1995 (2010), 1007.4785
- [23] P.G. Gu, D.N.C. Lin, P.H. Bodenheimer, ApJ, **588**, 509 (2003), arXiv:astro-ph/0303362
- [24] P. Hut, A&A, **99**, 126 (1981)
- [25] P.P. Eggleton, L.G. Kiseleva, P. Hut, ApJ, **499**, 853 (1998), arXiv:astro-ph/9801246
- [26] M. Gillon, B. Smalley, L. Hebb, D.R. Anderson, A.H.M.J. Triaud, C. Hellier, P.F.L. Maxted, D. Queloz, D.M. Wilson, A&A, **496**, 259 (2009), 0812.1998
- [27] M. López-Morales, S. Seager, ApJ, **667**, L191 (2007), 0708.0822
- [28] I.A.G. Snellen, E. Covino, MNRAS, **375**, 307 (2007), arXiv:astro-ph/0611877
- [29] E.J.W. de Mooij, I.A.G. Snellen, A&A, **493**, L35 (2009), 0901.1878
- [30] E.J.W. de Mooij, R.J. de Kok, S.V. Nefs, I.A.G. Snellen, A&A, **528**, A49+ (2011), 1103.0035